https://doi.org/10.5194/acp-2019-875
Preprint. Discussion started: 8 November 2019

Atmospheric Chemistry and Physics Discussions

Ozone Pollution over China and India: Seasonality and Sources

Meng Gao[1,2], Jinhui Gao[3], Bin Zhu[4], Rajesh Kumar[5], Xiao Lu[2], Shaojie Song[2], Yuzhong Zhang[2], Peng Wang[6], Gufran Beig[7], Jianlin Hu[8], Qi Ying[6], Hongliang Zhang[9], Peter Sherman[10], and Michael B McElroy[2,10]

1 Department of Geography, Hong Kong Baptist University, Hong Kong SAR, China
2 John A. Paulson School of Engineering and Applied Sciences, Harvard University, Cambridge, MA, United States
3 Department of Ocean Science and Engineering, Southern University of Science and Technology, Shenzhen, China
4 Key Laboratory for Aerosol-Cloud-Precipitation of China Meteorological Administration, Nanjing University of Information Science and Technology, Nanjing, China
5 National Center for Atmospheric Research, Boulder, CO, USA
6 Zachry Department of Civil Engineering, Texas A&M University, College Station, TX 77843-3136, USA
7 Indian Institute of Tropical Meteorology, Pune, India
8 School of Environmental Science and Engineering, Nanjing University of Information Science & Technology, 219 Ningliu Road, Nanjing 210044, China
9 Department of Environmental Science and Engineering, Fudan University, Shanghai 200438, China
10 Department of Earth and Planetary Sciences, Harvard University, Cambridge, MA, United States

Correspondence: Meng Gao (mmgao2@hkbu.edu.hk) and Michael B. McElroy (mbm@seas.harvard.edu)

https://doi.org/10.5194/acp-2019-875
Preprint. Discussion started: 8 November 2019

Atmospheric Chemistry and Physics Discussions

Abstract

A regional fully coupled meteorology-chemistry Weather Research and Forecasting model with Chemistry (WRF-Chem) was employed to study the seasonality of ozone (O_3) pollution and its sources in both China and India. Observations and model results suggest that O_3 in the North China Plain (NCP), Yangtze River Delta (YRD), Pearl River Delta (PRD) and India exhibit distinctive seasonal features, which are linked to the influence of summer monsoons. Through a factor separation approach, we examined the sensitivity of O_3 to individual anthropogenic, biogenic, and biomass burning emissions. We found that summer O_3 formation is more sensitive to industrial sources than to other source sectors for China, while the transport vehicle sector is more important in all seasons for India. For India, in addition to transport, the residential sector also plays an important role in winter when O_3 concentrations peak. Tagged simulations suggest that sources in east China play an important role in the formation of the summer O_3 peak in the NCP, but sources from Northwest China should not be neglected to control summer O_3 in the NCP. For the YRD region, prevailing winds and cleaner air from the ocean in summer lead to reduced transport from polluted regions, and the major source region in addition to local sources is Southeast China. For the PRD region, the upwind region is replaced by contributions from polluted east China as autumn approaches, leading to an autumn peak. The major upwind regions in autumn for the PRD are YRD (11%) and Southeast China (10%). For India, sources in North India are more important than sources in the south. These analyses emphasize the relative importance of source sectors and regions as they change with seasons, providing important implications for O_3 control strategies.

https://doi.org/10.5194/acp-2019-875
Preprint. Discussion started: 8 November 2019

Atmospheric Chemistry and Physics Discussions

1 Introduction

Tropospheric ozone (O_3) is the third most potent greenhouse gas in the atmosphere (*Pachauri and Reisinger, 2007*), an important surface air pollutant, and the major source of the hydroxyl radical (a key oxidant playing an essential role in atmospheric chemistry). With the rapid growth of industrialization, urbanization and transportation activities, emissions of O_3 precursors (nitrogen oxides and volatile organic compounds) in both China and India have increased significantly since 2000 (*De Smedt et al., 2010; Duncan et al., 2014; Hilboll et al., 2013; Kurokawa et al., 2013; Ohara et al., 2007; Stavrakou et al., 2009; Zheng et al., 2018*). Increasing concentrations of O_3 precursors have led to emerging and far-flung O_3 pollution, threatening health and food security (*Chameides et al., 1994; Malley et al., 2018*). The decrease in crop yield resulting from the increase in surface O_3 would have been sufficient to feed 95 million people in India (*Ghude et al., 2014*).

Great efforts have been devoted to improving understanding of exceptionally high concentrations (*Wang et al., 2006*) and the increasing trend in O_3 for both China and India (*Beig et al., 2007; Cheng et al., 2016; Ghude et al., 2008; Lu et al., 2018a; Ma et al., 2016; Saraf and Beig, 2004; Xu et al., 2008*). Strong but distinctive seasonal variations of O_3 observed in in India and China have been linked to higher emissions of precursor gases (*Lal et al., 2000*), stratospheric intrusions (*Kumar et al., 2010*), and the summer monsoon (*Kumar et al., 2010; Lu et al., 2018b; Wang et al., 2017*). The contributions of individual economic sectors and source regions were reported based on sensitivity simulations and source apportionment techniques (*J. Gao et al., 2016; Li et al., 2008; Li et al., 2016; Li et al., 2012; Lu et al., 2019; Wang et al., 2019*). With respect to the enhanced concentrations of O_3 over the past years, *Sun et al. (2019)* attributed this to elevated emissions of anthropogenic VOCs, while *Li et al. (2019)* argued that an inhibited aerosol sink for hydroperoxyl radicals induced by decreased $PM_{2.5}$ over 2013-2017 played a more important role in the NCP.

Despite this progress, the seasonal behaviors of O_3 in different regions greatly differ, yet have not been intercompared and the underlying causes have not been comprehensively explored. In addition, previous source apportionment studies focused on specific regions or episodes, and the policy implications drawn from these studies might not be applicable for other regions and seasons. It is both of interest and of significance to understand the similarities and differences

https://doi.org/10.5194/acp-2019-875
Preprint. Discussion started: 8 November 2019

Atmospheric Chemistry and Physics Discussions

between O_3 pollution in China and India, the two most polluted and most populous countries in the world.

The present study uses a fully online coupled meteorology-chemistry model (WRF-Chem) to examine the general seasonal features of O_3 pollution, and its sources derived from economic sectors and regions over both China and India. Sect. 2 describes the air quality model and measurements. We examine then in Sect. 3 how the model captures the spatial and temporal variations of O_3 and relevant precursors. Sect. 4 presents general seasonal features of O_3 pollution, and the relative importance of both economic sectors and source regions. Results are summarized in Sect. 5.

2 Model and data

2.1 WRF-Chem model and configurations

The fully online coupled meteorology-chemistry model WRF-Chem (*Grell et al., 2005*) was employed in this study using the CBMZ (Carbon Bond Mechanism version Z, *Zaveri and Peters, 1999*) photochemical mechanism and the MOSAIC (Model for simulating aerosol interactions and chemistry, *Zaveri et al., 2008*) aerosol chemistry module. The model was configured with a horizontal grid spacing of 60km with 27 vertical layers (from the surface to 10 hPa), covering East and South Asia (Fig. 1). The selected physical parameterization schemes follow the settings documented in *M. Gao et al. (2016)*. Meteorological initial and boundary conditions were obtained from the 6-hourly FNL (final analyses, *NCEP, 2000*) global analysis data with 1.0°×1.0° resolution. The four-dimensional data assimilation (FDDA) technique was applied to limit errors in simulated meteorology. Horizontal winds, temperature and moisture were nudged at all vertical levels. Chemical initial and boundary conditions were provided using MOZART-4 (*Emmons et al., 2010*) global simulations of chemical species.

Monthly anthropogenic emissions of SO_2, NO_x, CO, NMVOCs (Non-methane Volatile Organic Compounds), NH_3, $PM_{2.5}$, PM_{10}, BC (black carbon) and OC (organic carbon) were taken from the MIX 2010 inventory (*Li et al., 2017*), a mosaic Asian anthropogenic emission inventory covering both China and India. In this study, the emissions in China were updated with the MEIC (Multi-resolution Emission Inventory for China, http://www.meicmodel.org/) inventory for year 2012. The MIX inventory was prepared considering five economic sectors on a

https://doi.org/10.5194/acp-2019-875
Preprint. Discussion started: 8 November 2019

Atmospheric Chemistry and Physics Discussions

137 0.25°×0.25° grid: power, industrial, residential (heating, combustion, solvent use, and waste
138 disposal), transportation and agriculture. For India, SO_2, BC, OC, and power plant NO_x
139 emissions were taken from the inventory developed by the Argonne National Laboratory
140 (ANL), with the REAS (Regional Emission inventory in Asia) inventory used to supplement
141 for missing species. Speciation mapping of VOCs emissions follows the speciation framework
142 documented in *Li et al. (2014)* and *Gao et al. (2018)*. The MEGAN (Model for Emissions of
143 Gases and Aerosols from Nature, *Guenther et al., 2012*) model version 2.1 was used to generate
144 biogenic emissions online. Biomass burning emissions were obtained from the 4th generation
145 global fire emissions database (GFED4, *Giglio et al., 2013*). For China, industrial and power
146 sectors are the largest two contributors to NO_x emissions, while industrial sector emits the
147 largest amounts of NMVOCs (*Li et al., 2017*). For India, transportation and power sectors
148 produce the largest amounts of NO_x, while residential and transportation sectors are the largest
149 two contributors to NMVOCs emissions (*Li et al., 2017*). China's biogenic emissions of VOCs
150 are estimated to be higher than anthropogenic sources (*Li and Xie, 2014; Wei et al., 2011*).
151
152 **2.2 Ozone tagging method and setting of source regions**
153 O_3 observed in a particular region is a mixture of O_3 formed by reactions of NO_x with VOCs
154 emitted at different locations and time. The O_3 tagging method has the capability to apportion
155 contributions of different source regions to O_3 concentrations observed in particular regions.
156 The present study adopted the ozone tagging method implemented in WRF-Chem by *J. Gao et*
157 *al. (2017)*, which is similar to the Ozone Source Apportionment Technology (OSAT, *Yarwood*
158 *et al., 1996*) approach implemented in the Comprehensive Air Quality Model with extensions
159 (CAMx). Both O_3 and its precursors from different source regions are tracked as independent
160 variables. The ratio of formaldehyde to reactive nitrogen oxides ($HCHO/NO_y$) was used as
161 proposed by *Sillman (1995)* to decide whether the grid cell is under NO_x or VOC limited
162 conditions, and then different equations for these two conditions were selected to calculate total
163 O_3 chemical production. A detailed description of the technique is provided in *J. Gao et al.*
164 *(2017)*.
165 The O_3 tagging method attributes production of O_3 and its precursors to individual geographic
166 areas. We divided the entire modeling domain into 23 source regions, which were classified

https://doi.org/10.5194/acp-2019-875
Preprint. Discussion started: 8 November 2019

Atmospheric Chemistry and Physics Discussions

mainly using the administrative boundaries of provinces. In eastern China, each province was considered as a source region, while provinces in northeastern, northwestern, and southwestern China were lumped together (Fig. S1). India was divided into two source regions (north and south), and other countries were considered separately as a whole (Fig. S1). Additionally, the chemical boundaries provided by MOZART-4 were adopted to specify inputs of O_3, and the initial condition was tracked also as an independent source. The names of all source groupings are indicated in Fig. S1.

2.3 Experiment design

To quantify the sectoral contributions to O_3, a factor separation approach (FSA) was applied to differentiate two model simulations: one with all emission sources considered, and the other with some emission sources excluded. Table 1 summarizes the different sets of simulations conducted in this study. In addition to the control case, a series of sensitivity studies was performed, in which industrial, residential, transport, power, biogenic and fire emissions were separately excluded (Table 1). For each case, the entire year of 2013 was simulated.

2.4 Measurements

Surface air pollutants in China are measured and recorded by the Ministry of Environmental Protection (MEP), and the data are accessible on the China National Environmental Monitoring Center (CNEMC) website (http://106.37.208.233:20035/). This nationwide network was initiated in January 2013, and this dataset was used to evaluate model performance. This dataset has been extensively employed in previous studies to understand the spatial and temporal variations of air pollution in China (*Hu et al., 2016; Lu et al., 2018a*), and to reduce uncertainties in estimates of health and climate effects (*M. Gao et al., 2017*). Measurements of air pollutants from the MAPAN network (Modeling of Atmospheric Pollution and Networking) set up by the Indian Institute of Tropical Meteorology (IITM) under project SAFAR (System of Air Quality and weather Forecasting And Research) (*Beig et al., 2015*) were used in the present study to evaluate the model performance over India. To further evaluate how the model performed in capturing the vertical distributions of O_3, we used data from ozonesonde records obtained from the World Ozone and Ultraviolet Radiation Data Center website

https://doi.org/10.5194/acp-2019-875
Preprint. Discussion started: 8 November 2019

Atmospheric Chemistry and Physics Discussions

(https://woudc.org/data/dataset_info.php?id=ozonesonde). Fig. 1 displays the locations of the relevant surface and ozonesonde observation sites. We evaluated also the spatial distribution of NO_2 columns using the KNMI-DOMINO products of tropospheric NO_2 column (www.temis.nl). We excluded pixels observed under cloudy conditions (cloud fractions greater than 0.2) in the comparison.

3 Model evaluation

We evaluated the spatial distribution of simulated seasonal mean (winter months include January, February and December; spring months include March, April and May; summer months include June, July and August; Autumn months include September, October, and November) O_3 concentrations by comparing model results with observations (filled circles in Fig. 2) for 62 cities in China and India. The model captures the spatiotemporal patterns of O_3 in east China, with lower values in fall (Fig. 2d) and winter (Fig. 2a), and enhanced levels in spring (Fig. 2b) and summer (Fig. 2c). However, O_3 concentrations are overestimated by the model in central, northwest and southwest China for all seasons (Fig. 2). *Hu et al. (2016)* reported also that their model tends to predict higher O_3 concentrations for these regions. Comparisons between simulated and observed diurnal variations suggest that nighttime O_3 concentrations inferred by the model are higher than observation (*Hu et al., 2016*). During nighttime, O_3 concentrations are depressed through reaction with NO (NO_x titration). Fig. S2 indicates that modeled NO_2 column values in central, northwest and southwest China are not as high as observed, suggesting underestimation of NO_x emissions and less nighttime consumption of O_3 by NO. The simulated magnitudes of O_3 in India are generally consistent with observations, though lower in central India.

We conducted a further site-by-site evaluation of monthly mean O_3 concentrations, and grouped stations into four major densely-populated regions, namely North China Plain (NCP), Yangtze River Delta (YRD), Pearl River Delta (PRD), and India. The grouping categories follow the descriptions documented in *Hu et al. (2016)*. The seasonality of observed O_3 concentrations is reproduced well in these four regions (Fig. 3), although concentrations are underestimated in the NCP in spring. Stronger NO_x titration (underestimation of O_3 during the night, figure not shown), as indicated by the overestimation of NO_2 column over the NCP in

https://doi.org/10.5194/acp-2019-875
Preprint. Discussion started: 8 November 2019


Atmospheric Chemistry and Physics Discussions

spring (Fig. S2), is the most likely cause for these underestimations of O_3. The correlation coefficients between model and observations range between 0.84 and 0.98. Fig. 3 suggests also that the seasonal behavior of O_3 in these four major regions exhibits distinctive patterns, discussed in detail in Sect. 4.

In this work, ozonesonde measurements from the Hong Kong Observatory (HKO), Japan Meteorological Agency (JMA), and the Hydrometeorological Service of S.R. Vietnam (HSSRV) (locations marked in purple in Fig. 1) were used. Wintertime near-surface O_3 concentrations are overestimated for HKO (Fig. S3), while vertical variations are satisfactorily captured by the model.

Several issues are revealed through comparisons against measurements from multiple platforms. Comparisons of near-surface O_3 precursors suggest that CO concentrations are underestimated in all the regions, which could be explained by an underestimate of CO emissions (*Wang et al., 2011*). The coarse grid resolution of the model might provide another reason for this underestimation, as the observation sites in China are located mostly in urban areas. Underestimates of CO concentrations are reported also for many sites in India (*Hakim et al., 2019*). The effects of underestimated CO on O_3 were found to be small, but the underestimation of CO may lead to bias in methane lifetime (*Strode et al., 2015*), which is beyond the discussion of regional pollution in this study. Simulated NO_2 concentrations are slightly overestimated in the NCP but are underestimated in the PRD (Fig. S3), consistent with the comparison with satellite NO_2 columns (Fig. S2). However, the model still captures the seasonal behavior of O_3 in different regions, and we do not expect the model biases to change the major findings of the present study.

4 Seasonality, source sectors and source regions

4.1 Seasonality of surface O_3 in different regions

Comparisons between modeled and observed near-surface O_3 concentrations for different regions suggest distinctive seasonal patterns (Fig. 3). Over the NCP, near-surface O_3 exhibits an inverted V-shaped pattern, with maximum O_3 concentrations in summer, minimum in winter (Fig. 3). Over the YRD, O_3 presents a bridge shape, with relatively higher concentrations in spring, summer and autumn (Fig. 3). O_3 concentrations over the PRD peak in autumn, with a

https://doi.org/10.5194/acp-2019-875
Preprint. Discussion started: 8 November 2019

Atmospheric Chemistry and Physics Discussions

257 minimum in summer (Fig. 3). Similarly, O_3 over India exhibits a minimum in summer, with
258 highest concentrations in winter (Fig. 3).
259 China and India are influenced largely by monsoonal climates (*Wang et al., 2001*), and the
260 seasonality of O_3 in different regions is affected by wind pattern reversals related to the winter
261 and summer monsoon systems (*Lu et al., 2018*). Various monsoon indices have been proposed
262 to describe the major features of the Asian monsoon, based on pressure, temperature, and wind
263 fields, etc. In the present study, we adopted the dynamical normalized seasonality monsoon
264 index (DNSMI) developed by *Li and Zeng (2002)* to explore the influence of monsoon intensity
265 on the seasonal behavior of O_3 in the boundary layer in different regions of China and India.
266 DNSMI is defined as follows:

267 $$DNSMI = \frac{\|\overline{V_1} - V_i\|}{\bar{V}} - 2$$

268 in which V_1 and V_i represent the wind vectors in January, and wind vectors in month i,
269 respectively. $\bar{V}$ denotes the mean of wind vectors in January and July. The norm of a given
270 variable is defined as:

271 $$\|A\| = (\int\int |A|^2 dS)^{\frac{1}{2}}$$

272 where S represents the spatial area of each model grid cell. More detailed information on the
273 definition is presented in *Li and Zeng (2002)*.
274 This definition of monsoon focuses on wind vectors, representing the intensity of wind
275 direction alternation from winter to summer. In winter, northwesterly winds are predominant,
276 then higher DNSMI values indicate stronger alternation of wind directions. For example,
277 DNSMI values are higher than 5 in coastal regions of South China and most environments in
278 India (Fig. 4c), suggesting that these regions are influenced largely by the summer monsoon.
279 Over the ocean, DNSMI increases as spring approaches, reaching a maximum in summer (Fig.
280 4). Over land, the magnitude of DNSMI decreases, and relatively large values are found only
281 in coastal regions (Fig. 4). The alternation of wind vectors from winter to summer results also
282 in changes in upwind areas, modulating the severity of O_3 pollution. In summer, the southerly
283 winds containing clean maritime air masses, serve to reduce the intensity of pollution in regions
284 that are affected largely by the summer monsoon (e.g., most regions over India, and coastal
285 regions of China). Besides, cloudy and rainy conditions associated with the summer monsoon

https://doi.org/10.5194/acp-2019-875
Preprint. Discussion started: 8 November 2019

Atmospheric Chemistry and Physics Discussions

are not conducive to photochemical production of O_3 (Tang et al., 2013).

North China is influenced less than South China and East China by the summer monsoon as suggested by DNSMI values lower than 0.5 as shown in Fig. 4c, and weather conditions favor O_3 formation in summer (higher temperature and stronger solar radiation). As a result, O_3 concentrations in the NCP peak in summer, exhibiting an inverted V-shaped pattern (Fig. 3a). The YRD region is affected moderately by the summer monsoon, with DNSMI values greater than 0.6 (Fig. 4c). The upwind sources for the YRD in summer include both polluted (south China) and clean (ocean) regions. Thus, the inhibition of O_3 formation in the YRD due to the summer monsoon does not lead to the annual minima in summer. Because of the favorable weather conditions (increasing temperature and solar radiation, and low precipitation) in spring and autumn, the seasonality of O_3 in the YRD exhibits a bridge shape, consistent with previous observations within this region (*Tang et al., 2013*). In addition, southerly winds might bring O_3 and its precursors from the YRD region in summer (Fig. 4c), which will be further quantified in Sect. 4.3. For India and the PRD region, the alternation of wind fields begins as spring approaches (Fig. 4). As a result, O_3 concentrations decline in response to input of cleaner air from the ocean. As summer arrives, the intensity of the monsoon reaches its maximum (Fig. 4c) and concentrations of O_3 in both India and South China decline to reach their annual minima (Fig. 3c and Fig. 3d). As wind direction changes over the east coast of China from summer to autumn, O_3 peaks in autumn in South China can be attributed also to the outflow of O_3 and its precursors from the NCP and YRD regions (Fig. 4d). This contribution will be discussed further also in Sect. 4.3.

4.2 O_3 sensitivity to emissions from individual source sectors

O_3 in the troposphere is formed through complex nonlinear processes involving emissions of NO_x and VOCs from various anthropogenic, biogenic, and biomass burning sources. We illustrate in Fig. 5 the sensitivity of seasonal mean O_3 concentrations in both China and India to individual source sectors, patterns that offer important implications for seasonal O_3 control strategies in some highly polluted regions.

For China, summer O_3 formation is more sensitive to industrial sources than to other anthropogenic sources, including power, residential, and transport (Fig. 5c). Emissions from

https://doi.org/10.5194/acp-2019-875
Preprint. Discussion started: 8 November 2019


Atmospheric Chemistry and Physics Discussions

316 the industrial sector are responsible for an enhancement of O_3 concentrations by more than 10
317 ppb in east China in summer (Fig. 5c). Using a similar approach, *Li et al. (2017)* reported that
318 the contribution to O_3 from industrial sources exceeded 30 μg/m^3 (~15 ppb) in highly
319 industrialized areas, including Hebei, Shandong, Zhejiang, etc. during an episode in May. *Li et*
320 *al. (2016)* concluded that the industrial sector plays the most important role for O_3 formation
321 in Shanghai, accounting for more than 35% of observed concentrations. Adopting a source-
322 oriented chemical transport model, *Wang et al., (2019)* demonstrated that the industrial source
323 contributes 36%, 46%, and 29% to non-background O_3 in Beijing, Shanghai and Guangdong,
324 respectively.
325 In east China, O_3 formation in winter, spring, and autumn reflects negative sensitivity to the
326 transport and power sectors (Fig. 5). These two sectors dominate emissions of NO_x in China
327 (*Li et al., 2017*). Removing these sectors would lead to increases in O_3 in VOC-limited regions
328 of east China in winter, spring and fall (less biogenic emissions of VOCs in these seasons, *Fu*
329 *et al., 2012*). Urban regions in China are still VOC-limited (*Fu et al., 2012; Jin et al., 2017*) in
330 summer, leading to negligible or negative sensitivity to the transport and power sectors as
331 shown in Fig. 5g and Fig 5o. In other regions of east China, removing transport and power
332 sources would lead to an increase in O_3 concentrations by about 4 ppb in summer. The
333 sensitivity of O_3 concentrations to the residential sector in spring and autumn displays
334 appreciable magnitudes in the YRD, where O_3 peaks in autumn (Fig. 5).
335 Including biogenic emissions results in an increase in summer mean O_3 concentrations by more
336 than 20 ppb in east China (Fig. 5s). Using a similar approach, *Li et al. (2018)* found that
337 biogenic emissions contributed 8.2 ppb in urban Xi'an. Other source apportionment studies
338 indicate that the contribution of biogenic emissions to O_3 formation is about 20% in China (*Li*
339 *et al., 2016; Wang et al., 2019*). The enhancements due to biogenic emissions are larger over
340 south China during winter, and the significantly impacted regions extend northwards in spring
341 and autumn (Fig. 5q-5t). Biomass burning emissions lead to relatively lower O_3 enhancements
342 over China in winter, but are responsible for an appreciable contribution to O_3 pollution (~7
343 ppb) in east China in summer (Fig. 5w). *Li et al. (2016)* suggested that biomass burning sources
344 contribute about 4% to O_3 formation in the YRD region in summer. The enhancement due to
345 biomass burning estimated by *Lu et al. (2019)* using a different model indicates lower values

https://doi.org/10.5194/acp-2019-875
Preprint. Discussion started: 8 November 2019


Atmospheric Chemistry and Physics Discussions

in east China.

For India, O_3 formation is most sensitive to the transport vehicle sector (~8 ppb) in all seasons, slightly higher than it is to the biogenic source (Fig. 5m-5p). Among other sectors, the sensitivity of O_3 formation to the residential sector is significant in winter as residential sector emits the largest amount of NMVOCs (*Li et al., 2017*), while the influence of biomass burning emissions is negligible.

Our results highlight the importance of industrial sources in O_3 formation in east China, consistent with the conclusions of *Li et al.* (*2017*). The significance of other sectors demonstrated by *Li et al.* (*2017*), especially transport and biogenic emissions, disagrees with the current finding. Conclusions from *Li et al. (2017)* rely on simulations of a one-week episode in May, while our results provide more information considering different seasons and different highly polluted regions.

4.3 O_3 contribution from individual source regions

The sensitivity of O_3 pollution to individual source sectors discussed in the previous section provides a quantitative understanding of the relative importance of individual source sectors. Additionally, information on the contribution of individual source regions to O_3 pollution should provide useful inputs for O_3 control strategies. Because of the large computational costs of sensitivity simulations, we employed the tagging method to examine contributions to O_3 pollution from individual source regions. Fig. 6 presents monthly mean concentrations of O_3 averaged over the NCP, YRD, PRD and India, with contributions from individual source regions.

The NCP region is influenced largely by sources outside China, especially in wintertime, which might be attributed to less local production and a longer O_3 lifetime in winter. In winter, sources outside China are responsible for more than 75% of O_3 formation in the NCP region. However, this contribution declines to about 50% as summer approaches. Using the tagged tracer method with a global chemical transport model, *Nagashima et al. (2010)* suggested that sources outside China contributed about 60% and 40% to surface O_3 in North China in spring and summer, respectively. Our estimate for the contributions of sources outside China in these two seasons suggests slightly higher values: 73% and 51% (Table 2). In summer, NCP local sources

https://doi.org/10.5194/acp-2019-875
Preprint. Discussion started: 8 November 2019


Atmospheric Chemistry and Physics Discussions

contribute about 31%, with additional 8% from Northwestern China.

For the YRD region, local emissions contribute 32% to O_3 formation in summer, but the contribution declines by 8% in spring and autumn (Table 2). The contribution of sources outside China decreases greatly in summer (46%), leading to a small summer O_3 trough. The source apportionment results in *Nagashima et al. (2010)* also indicated that the contribution of sources outside China to O_3 in the Yangtze River Basin decreases significantly from spring to summer (44% to 30%). The relatively lower contribution from sources outside China is associated with the prevailing winds and cleaner air from the ocean in summer (Fig. 4c). In addition to local sources, we further identified the major source region for O_3 in the YRD region is the NCP in winter, spring and autumn (14%, 6% and 8%, respectively). In summer, the major source region of O_3 in the YRD region is Southeast China (10%). *J. Gao et al. (2016)* concluded that YRD local emissions contribute 13.6%-20.6% to daytime O_3 under different wind conditions, and the contribution of super regional sources (Outside) ranges from 32 to 34% in May. In Hangzhou (a megacity within YRD), source apportionment results reveal that long-range transport contributes 36.5% to daily maximum O_3 with the overall contribution dominated by local sources (*Li et al., 2016*).

O_3 concentrations in the YRD region are influenced largely by the summer monsoon, and the prevailing winds from the ocean result in a minimum contribution from polluted regions. The estimated contribution of sources outside China declines to 46% in summer, which agrees well with the number 47% inferred from *Nagashima et al. (2010)*. *Li et al. (2012)* applied the OSAT tool in the CAMx model to apportion O_3 sources in south China, and reported that super-regional sources contributed 55% and 71% to monthly mean O_3 in summer and autumn, respectively. They pointed out also that regional and local sources play more important roles in O_3 pollution episodes (*Li et al., 2002*). The contribution of local source peaks in summer (41%) exceeds the local contribution in the NCP and YRD regions. As discussed in Sect. 4.1, the outflow of O_3 and its precursors from the NCP and YRD regions might play important roles in peak autumn O_3 in the YRD (Fig. 4d), as wind direction switches from summer to autumn. We identified the major upwind regions for the PRD in autumn as YRD (11%) and Southeast China (10%). From summer to autumn, the contribution of YRD sources to the PRD increases from 2% to 11%. For India, O_3 concentrations are dominated by sources outside India, and

https://doi.org/10.5194/acp-2019-875
Preprint. Discussion started: 8 November 2019

Atmospheric Chemistry and Physics Discussions

sources in North India (Fig. 6d). In winter, sources outside India contribute 49%, while sources in North India contribute 38%.

The estimated contributions of sources outside China to O_3 pollution in receptor regions exhibit slightly higher values than the values inferred from studies using global models (*Nagashima et al., 2010; Wang et al., 2011*). This might be related partly to the inconsistency between simulations from the applied regional model and boundary conditions from another global model. Global chemical transport models usually show better skills in simulating transboundary pollution. In addition, the current study focuses on seasonal mean (both daytime and nighttime) O_3 while many previous studies investigate sources of 8-h or daily maximum O_3. As illustrated in *Li et al. (2016)*, the dominant contribution to nighttime O_3 is associated with long-range transport. All of these factors contribute to uncertainties in the results of source apportionment, but should not downplay the significance of current findings in terms of policy implications.

5 Summary

In this study, we used a fully coupled regional meteorology-chemistry model with a horizontal grid spacing of 60 km × 60 km to study the seasonality and characteristics of sources of O_3 pollution in highly polluted regions in both China and India. Both observations and model results indicate that O_3 in the NCP, YRD, PRD, and in India display distinctive seasonal features. Surface concentrations of O_3 peak in summer in the NCP, in spring in the YRD, in autumn in the PRD and in winter in India. These distinct seasonal features for different regions are linked to the intensity of the summer monsoon, to sources, and to atmospheric transport.

With confidence in the model's ability to reproduce the major features of O_3 pollution, we examined the sensitivity of O_3 pollution to individual anthropogenic emission sectors, and to emissions from biogenic sources and from burning of biomass. We found that production of O_3 in summer is more sensitive to industrial sources than to other source sectors for China, while the transport vehicle sector is more important for all seasons in India. For India, in addition to transport, the residential sector also plays an important role in winter when O_3 concentrations peak. These differences in conditions between China and India suggest differences in control strategies on economic sectors should be implemented to minimize resulting pollution.

https://doi.org/10.5194/acp-2019-875
Preprint. Discussion started: 8 November 2019

Atmospheric Chemistry and Physics Discussions

Tagged simulations suggest that sources in east China play an important role in the formation of the summer O_3 peak in the NCP, and sources from Northwest China should not be neglected to control summer O_3 in the NCP. For the YRD region, prevailing winds and cleaner air from the ocean in summer lead to reduced transport from polluted regions, and the major source region in addition to local sources is Southeast China. For the PRD region, the upwind region is replaced by contributions from polluted east China as autumn approaches, leading to an autumn peak. The major upwind regions in autumn for the PRD are YRD (11%) and Southeast China (10%). For India, sources in North India show larger contributions than sources in South India.

The focus of our analysis is on the seasonality of O_3 pollution and its sources in both China and India, with an emphasis on implications for O_3 control strategies. Most previous studies focused on the analysis of episodes or monthly means for a region, while the current study presents a more comprehensive picture. For the NCP region, O_3 concentrations peak in summer, during which industrial sources should be given higher priority. Besides local sources in the NCP, sources from Northwest China play also important roles. For the YRD region, O_3 concentrations in spring, summer and autumn are equally important, showing appreciable sensitivity to the industrial sources. In addition to local sources, sources from the NCP should be considered for control of O_3 in spring and autumn, while sources from Southeast China should be considered in summer. For the PRD region, O_3 concentrations peak in spring and autumn, during which reducing industrial and transport sources could be more effective. In both spring and autumn, sources from the YRD and Southeast China show appreciable contributions to O_3 pollution in the PRD. For India, O_3 pollution is more serious in winter, during which controlling residential and transport sources in North India could be more effective. Although large uncertainties remain in the tagged O_3 method, notably the inconsistency of transboundary simulation using regional models, the current findings are expected to provide useful insights on the relative importance of different source sectors and regions.

https://doi.org/10.5194/acp-2019-875
Preprint. Discussion started: 8 November 2019

Atmospheric Chemistry and Physics Discussions

4 figures are listed in the supplement.

Author contribution

M.G. and M.B.M designed the study; M.G. performed model simulations and analyzed the data with the help from J. G., B. Z., R. K., X. L., S. S., Y. Z., P. W., P. S.; G. B., J.H., Q.Y., H.Z. provided measurements. M.G. and M.B.M. wrote the paper with inputs from all other authors.

Data availability

The measurements and model simulations data can be accessed through contacting the corresponding authors.

Competing interests

The authors declare that they have no conflict of interests.

Acknowledgement

This work is supported by the Harvard Global Institute and special fund of State Key Joint Laboratory of Environment Simulation and Pollution Control (19K03ESPCT).

Reference

Beig, G., Gunthe, S. and Jadhav, D. B.: Simultaneous measurements of ozone and its precursors on a diurnal scale at a semi urban site in India, J. Atmos. Chem., 57(3), 239–253, doi:10.1007/s10874-007-9068-8, 2007.

Beig G., GAW Report No. 217, System of Air Quality Forecasting and Research (SAFAR-INDIA), World Meteorological Organization, 2015.

Chameides, W.L., Kasibhatla, P.S., Yienger, J., Levy II, H.: Growth of Continental-scale Metro-Agro-Plexes, Regional Ozone Pollution, and World Food Production, Science (80-.)., 264(APRIL), 1994.

Cheng, N., Li, Y., Zhang, D., Chen, T., Sun, F., Chen, C. and Meng, F.: Characteristics of Ground Ozone Concentration over Beijing from 2004 to 2015: Trends, Transport, and Effects of Reductions, Atmos. Chem. Phys. Discuss., 1(x), 1–21, doi:10.5194/acp-2016-508, 2016.

https://doi.org/10.5194/acp-2019-875
Preprint. Discussion started: 8 November 2019

500 De Smedt, I., Stavrakou, T., Mller, J. F., Van Der A, R. J. and Van Roozendael, M.: Trend detection
501 in satellite observations of formaldehyde tropospheric columns, Geophys. Res. Lett., 37(18),
502 doi:10.1029/2010GL044245, 2010.
503
504 Duncan, B.N., Lamsal, L.N., Thompson, A.M., Yoshida, Y., Lu, Z., Streets, D.G., Hurwitz, M.M.
505 and Pickering, K.E.: A space-based, high-resolution view of notable changes in urban NOx
506 pollution around the world (2005–2014), J. Geophys. Res. Atmos., 121(2), pp.976-996, 2016.
507
508 Emmons, L. K., Walters, S., Hess, P. G., Lamarque, J.-F., Pfister, G. G., Fillmore, D., Granier, C.,
509 Guenther, a., Kinnison, D., Laepple, T., Orlando, J., Tie, X., Tyndall, G., Wiedinmyer, C.,
510 Baughcum, S. L. and Kloster, S.: Description and evaluation of the Model for Ozone and
511 Related chemical Tracers, version 4 (MOZART-4), Geosci. Model Dev., 3(1), 43–67,
512 doi:10.5194/gmd-3-43-2010, 2010.
513
514 Fu, J. S., Dong, X., Gao, Y., Wong, D. C. and Lam, Y. F.: Sensitivity and linearity analysis of ozone
515 in East Asia: The effects of domestic emission and intercontinental transport, J. Air Waste
516 Manage. Assoc., 62(March 2015), 1102–1114, doi:10.1080/10962247.2012.699014, 2012.
517
518 Gao, J., Zhu, B., Xiao, H., Kang, H., Hou, X., Yin, Y., Zhang, L. and Miao, Q.: Diurnal variations
519 and source apportionment of ozone at the summit of Mount Huang, a rural site in Eastern China,
520 Environ. Pollut., 222, 513–522, doi:10.1016/j.envpol.2016.11.031, 2017.
521
522 Gao, J., Zhu, B., Xiao, H., Kang, H., Hou, X. and Shao, P.: A case study of surface ozone source
523 apportionment during a high concentration episode, under frequent shifting wind conditions
524 over the Yangtze River Delta, China, Sci. Total Environ., 544, 853–863,
525 doi:10.1016/j.scitotenv.2015.12.039, 2016.
526
527 Gao, M., Carmichael, G. R., Wang, Y., Saide, P. E., Yu, M., Xin, J., Liu, Z. and Wang, Z.: Modeling
528 study of the 2010 regional haze event in the North China Plain, Atmos. Chem. Phys., 16(3),
529 1673–1691, doi:10.5194/acp-16-1673-2016, 2016.
530
531 Gao, M., Han, Z., Liu, Z., Li, M., Xin, J., Tao, Z., Li, J., Kang, J. E., Huang, K., Dong, X., Zhuang,
532 B., Li, S., Ge, B., Wu, Q., Cheng, Y., Wang, Y., Lee, H. J., Kim, C. H., Fu, J. S., Wang, T., Chin,
533 M., Woo, J. H., Zhang, Q., Wang, Z. and Carmichael, G. R.: Air quality and climate change,
534 Topic 3 of the Model Inter-Comparison Study for Asia Phase III (MICS-Asia III) - Part 1:
535 Overview and model evaluation, Atmos. Chem. Phys., 18(7), 4859–4884, doi:10.5194/acp-18-
536 4859-2018, 2018.
537
538 Gao, M., Saide, P. E., Xin, J., Wang, Y., Liu, Z., Wang, Y., Wang, Z., Pagowski, M., Guttikunda, S.
539 K. and Carmichael, G. R.: Estimates of Health Impacts and Radiative Forcing in Winter Haze
540 in Eastern China through Constraints of Surface PM2.5 Predictions, Environ. Sci. Technol.,
541 51(4), 2178–2185, doi:10.1021/acs.est.6b03745, 2017.
542
543 Ghude, S. D., Jena, C., Chate, D.M., Beig, G., Pfister, G.G., Kumar, R., Ramanathan, V.: Reductions

https://doi.org/10.5194/acp-2019-875
Preprint. Discussion started: 8 November 2019

in India's crop yield due to ozone, Geophys. Res. Lett., 41, 5685–5691, doi:10.1002/2014GL060930.Received, 2014.

Ghude, S. D., Jain, S. L., Arya, B. C., Beig, G., Ahammed, Y. N., Kumar, A. and Tyagi, B.: Ozone in ambient air at a tropical megacity, Delhi: Characteristics, trends and cumulative ozone exposure indices, J. Atmos. Chem., 60(3), 237–252, doi:10.1007/s10874-009-9119-4, 2008.

Giglio, L., Randerson, J. T. and Van Der Werf, G. R.: Analysis of daily, monthly, and annual burned area using the fourth-generation global fire emissions database (GFED4), J. Geophys. Res. Biogeosciences, 118(1), 317–328, doi:10.1002/jgrg.20042, 2013.

Grell, G. a., Peckham, S. E., Schmitz, R., McKeen, S. a., Frost, G., Skamarock, W. C. and Eder, B.: Fully coupled "online" chemistry within the WRF model, Atmos. Environ., 39(37), 6957–6975, doi:10.1016/j.atmosenv.2005.04.027, 2005.

Guenther, A. B., Jiang, X., Heald, C. L., Sakulyanontvittaya, T., Duhl, T., Emmons, L. K. and Wang, X.: The model of emissions of gases and aerosols from nature version 2.1 (MEGAN2.1): An extended and updated framework for modeling biogenic emissions, Geosci. Model Dev., 5(6), 1471–1492, doi:10.5194/gmd-5-1471-2012, 2012.

Hakim, Z. Q., Archer-Nicholls, S., Beig, G., Folberth, G. A., Sudo, K., Luke Abraham, N., Ghude, S., Henze, D. K. and Archibald, A. T.: Evaluation of tropospheric ozone and ozone precursors in simulations from the HTAPII and CCMI model intercomparisons-A focus on the Indian subcontinent, Atmos. Chem. Phys., 19(9), 6437–6458, doi:10.5194/acp-19-6437-2019, 2019.

Hilboll, A., Richter, A. and Burrows, J. P.: Long-term changes of tropospheric NO2 over megacities derived from multiple satellite instruments, Atmos. Chem. Phys., 13(8), 4145–4169, doi:10.5194/acp-13-4145-2013, 2013.

Hu, J., Chen, J., Ying, Q. and Zhang, H.: One-year simulation of ozone and particulate matter in China using WRF/CMAQ modeling system, Atmos. Chem. Phys., 16(16), 10333–10350, doi:10.5194/acp-16-10333-2016, 2016.

Jin, X., Fiore, A. M., Murray, L. T., Valin, L. C., Lamsal, L. N., Duncan, B., Folkert Boersma, K., De Smedt, I., Abad, G. G., Chance, K. and Tonnesen, G. S.: Evaluating a Space-Based Indicator of Surface Ozone-NOx-VOC Sensitivity Over Midlatitude Source Regions and Application to Decadal Trends, J. Geophys. Res. Atmos., 122(19), 10439–10461, doi:10.1002/2017JD026720, 2017.

Kumar, R., Naja, M., Venkataramani, S. and Wild, O.: Variations in surface ozone at Nainital: A high-altitude site in the central Himalayas, J. Geophys. Res. Atmos., 115(16), 1–12, doi:10.1029/2009JD013715, 2010.

Kurokawa, J., Ohara, T., Morikawa, T., Hanayama, S., Janssens-Maenhout, G., Fukui, T.,

https://doi.org/10.5194/acp-2019-875
Preprint. Discussion started: 8 November 2019

588 Kawashima, K. and Akimoto, H.: Emissions of air pollutants and greenhouse gases over Asian
589 regions during 2000-2008: Regional Emission inventory in ASia (REAS) version 2, Atmos.
590 Chem. Phys., 13(21), 11019–11058, doi:10.5194/acp-13-11019-2013, 2013.
591
592 Lal, S., Naja, M. and Subbaraya, B. H.: Seasonal variations in surface ozone and its precursors over
593 an urban site in India, Atmos. Environ., 34(17), 2713–2724, doi:10.1016/S1352-
594 2310(99)00510-5, 2000.Li, J., Wang, Z., Akimoto, H., Yamaji, K., Takigawa, M., Pochanart, P.,
595 Liu, Y., Tanimoto, H. and Kanaya, Y.: Near-ground ozone source attributions and outflow in
596 Central Eastern China during MTX2006, Atmos. Chem. Phys., 8(24), 7335–7351,
597 doi:10.5194/acp-8-7335-2008, 2008.
598
599 Li, J. and Zeng, Q.: A new monsoon index and the geographical distribution of the global monsoons,
600 Adv. Atmos. Sci., 20(2), 299–302, 2003.
601
602 Li, J., Wang, Z., Akimoto, H., Yamaji, K., Takigawa, M., Pochanart, P., Liu, Y., Tanimoto, H. and
603 Kanaya, Y.: Near-ground ozone source attributions and outflow in central eastern China during
604 MTX2006, Atmos. Chem. Phys., 8(24), pp.7335-7351, 2008.
605
606 Li, K., Jacob, D. J., Liao, H., Shen, L., Zhang, Q. and Bates, K. H.: Anthropogenic drivers of 2013–
607 2017 trends in summer surface ozone in China, Proc. Natl. Acad. Sci. U. S. A., 116(2), 422–
608 427, doi:10.1073/pnas.1812168116, 2019.
609
610 Li, L. Y. and Xie, S. D.: Historical variations of biogenic volatile organic compound emission
611 inventories in China, 1981-2003, Atmos. Environ., 95, 185–196,
612 doi:10.1016/j.atmosenv.2014.06.033, 2014.
613
614 Li, L., An, J. Y., Shi, Y. Y., Zhou, M., Yan, R. S., Huang, C., Wang, H. L., Lou, S. R., Wang, Q., Lu,
615 Q. and Wu, J.: Source apportionment of surface ozone in the Yangtze River Delta, China in the
616 summer of 2013, Atmos. Environ., 144, 194–207, doi:10.1016/j.atmosenv.2016.08.076, 2016.
617
618 Li, M., Zhang, Q., Streets, D. G., He, K. B., Cheng, Y. F., Emmons, L. K., Huo, H., Kang, S. C.,
619 Lu, Z., Shao, M., Su, H., Yu, X. and Zhang, Y.: Mapping Asian anthropogenic emissions of
620 non-methane volatile organic compounds to multiple chemical mechanisms, Atmos. Chem.
621 Phys., 14(11), 5617–5638, doi:10.5194/acp-14-5617-2014, 2014.
622
623 Li, M., Zhang, Q., Kurokawa, J. I., Woo, J. H., He, K., Lu, Z., Ohara, T., Song, Y., Streets, D. G.,
624 Carmichael, G. R., Cheng, Y., Hong, C., Huo, H., Jiang, X., Kang, S., Liu, F., Su, H. and Zheng,
625 B.: MIX: A mosaic Asian anthropogenic emission inventory under the international
626 collaboration framework of the MICS-Asia and HTAP, Atmos. Chem. Phys., 17(2), 935–963,
627 doi:10.5194/acp-17-935-2017, 2017.
628
629 Li, N., He, Q., Greenberg, J., Guenther, A., Li, J., Cao, J., Wang, J., Liao, H., Wang, Q. and Zhang,
630 Q.: Impacts of biogenic and anthropogenic emissions on summertime ozone formation in the
631 Guanzhong Basin, China, Atmos. Chem. Phys., 18(10), 7489–7507, doi:10.5194/acp-18-7489-

https://doi.org/10.5194/acp-2019-875
Preprint. Discussion started: 8 November 2019

2018, 2018.

Li, Y., Lau, A. K. H., Fung, J. C. H., Zheng, J. Y., Zhong, L. J. and Louie, P. K. K.: Ozone source apportionment (OSAT) to differentiate local regional and super-regional source contributions in the Pearl River Delta region, China, J. Geophys. Res. Atmos., 117(15), 1–18, doi:10.1029/2011JD017340, 2012.

Lu, X., Hong, J., Zhang, L., Cooper, O. R., Schultz, M. G., Xu, X., Wang, T., Gao, M., Zhao, Y. and Zhang, Y.: Severe Surface Ozone Pollution in China: A Global Perspective, Environ. Sci. Technol. Lett., 5(8), 487–494, doi:10.1021/acs.estlett.8b00366, 2018.

Lu, X., Zhang, L., Liu, X., Gao, M., Zhao, Y. and Shao, J.: Lower tropospheric ozone over India and its linkage to the South Asian monsoon, Atmos. Chem. Phys., 18(5), 3101–3118, doi:10.5194/acp-18-3101-2018, 2018.

Ma, Z., Xu, J., Quan, W., Zhang, Z., Lin, W. and Xu, X.: Significant increase of surface ozone at a rural site, north of eastern China, Atmos. Chem. Phys., 16(6), 3969–3977, doi:10.5194/acp-16-3969-2016, 2016.

Malley, C.: Tropospheric Ozone Assessment Report: Present-day tropospheric ozone distribution and trends relevant to vegetation. Elementa: Science of the Anthropocene, 2018.

Nagashima, T., Ohara, T., Sudo, K. and Akimoto, H.: The relative importance of various source regions on East Asian surface ozone, Atmos. Chem. Phys., 10(22), 11305–11322, doi:10.5194/acp-10-11305-2010, 2010.

NCEP, National Weather Service, NOAA & U.S. Department of Commerce. NCEP Final (FNL) Operational Model Global Tropospheric Analyses, continuing from July 1999. https://doi.org/10.5065/D6M043C6 (Research Data Archive at the National Center for Atmospheric Research, Computational and Information Systems Laboratory, 2000).

Ohara, T., Akimoto, H., Kurokawa, J., Horii, N., Yamaji, K., Yan, X. and Hayasaka, T.: An Asian emission inventory of anthropogenic emission sources for the period 1980-2020, Atmos. Chem. Phys., 7(16), 4419–4444, doi:10.5194/acp-7-4419-2007, 2007.

Pachauri, R.K. and Reisinger, A.: IPCC fourth assessment report. IPCC, Geneva, p.2007, 2007.

Saraf, N. and Beig, G.: Long-term trends in tropospheric ozone over the Indian tropical region, Geophys. Res. Lett., 31(5), n/a-n/a, doi:10.1029/2003gl018516, 2004.

Sillman, S.: The use of NOy, H2O2, and HNO3as indicators for ozone-NOx- hydrocarbon sensitivity in urban locations, J. Geophys. Res., 100(D7), 175–188, 1995.

Stavrakou, T., Müller, J. F., De Smedt, I., Van Roozendael, M., Van Der Werf, G. R., Giglio, L. and

https://doi.org/10.5194/acp-2019-875
Preprint. Discussion started: 8 November 2019

Guenther, A.: Evaluating the performance of pyrogenic and biogenic emission inventories against one decade of space-based formaldehyde columns, Atmos. Chem. Phys., 9(3), 1037–1060, doi:10.5194/acp-9-1037-2009, 2009.

Strode, S.A., Duncan, B.N., Yegorova, E.A., Kouatchou, J., Ziemke, J.R. and Douglass, A.R.: Implications of carbon monoxide bias for methane lifetime and atmospheric composition in chemistry climate models. Atmospheric chemistry and physics, 15(20), pp.11789-11805, 2015.

Sun, L., Xue, L., Wang, Y., Li, L., Lin, J., Ni, R., Yan, Y., Chen, L., Li, J., Zhang, Q. and Wang, W.: Impacts of meteorology and emissions on summertime surface ozone increases over central eastern China between 2003 and 2015, Atmos. Chem. Phys., 19(3), 1455–1469, doi:10.5194/acp-19-1455-2019, 2019.

Tang, H., Liu, G., Zhu, J., Han, Y. and Kobayashi, K.: Seasonal variations in surface ozone as influenced by Asian summer monsoon and biomass burning in agricultural fields of the northern Yangtze River Delta, Atmos. Res., 122, 67–76, doi:10.1016/j.atmosres.2012.10.030, 2013.

Wang, B., Wu, R. and Lau, K. M.: Interannual variability of the asian summer monsoon: Contrasts between the Indian and the Western North Pacific-East Asian monsoons, J. Clim., 14(20), 4073–4090, doi:10.1175/1520-0442(2001)014, 2001.

Wang, P., Chen, Y., Hu, J., Zhang, H. and Ying, Q.: Source apportionment of summertime ozone in China using a source-oriented chemical transport model, Atmos. Environ., 211(May), 79–90, doi:10.1016/j.atmosenv.2019.05.006, 2019.

Wang, T., Ding, A., Gao, J. and Wu, W. S.: Strong ozone production in urban plumes from Beijing, China, Geophys. Res. Lett., 33(21), doi:10.1029/2006GL027689, 2006.

Wang, T., Xue, L., Brimblecombe, P., Lam, Y. F., Li, L. and Zhang, L.: Ozone pollution in China: A review of concentrations, meteorological influences, chemical precursors, and effects, Sci. Total Environ., 575, 1582–1596, doi:10.1016/j.scitotenv.2016.10.081, 2017.

Wang, Y., Zhang, Y., Hao, J. and Luo, M.: Seasonal and spatial variability of surface ozone over China: Contributions from background and domestic pollution, Atmos. Chem. Phys., 11(7), 3511–3525, doi:10.5194/acp-11-3511-2011, 2011.

Wei, W., Wang, S., Hao, J. and Cheng, S.: Projection of anthropogenic volatile organic compounds (VOCs) emissions in China for the period 2010-2020, Atmos. Environ., 45(38), 6863–6871, doi:10.1016/j.atmosenv.2011.01.013, 2011.

Xu, X., Lin, W., Wang, T., Yan, P., Tang, J., Meng, Z. and Wang, Y.: Long-term trend of surface ozone at a regional background station in eastern China 1991-2006: Enhanced variability, Atmos. Chem. Phys., 8(10), 2595–2607, doi:10.5194/acp-8-2595-2008, 2008.

https://doi.org/10.5194/acp-2019-875
Preprint. Discussion started: 8 November 2019

Atmospheric Chemistry and Physics Discussions

720
721 Yarwood, G., Morris, R.E., Yocke, M.A., Hogo, H. and Chico, T.: Development of a methodology
722 for source apportionment of ozone concentration estimates from a photochemical grid
723 model. AIR & WASTE MANAGEMENT ASSOCIATION, PITTSBURGH, PA
724 15222(USA).[np], 1996.
725
726 Zaveri, R. a., Easter, R. C., Fast, J. D. and Peters, L. K.: Model for Simulating Aerosol Interactions
727 and Chemistry (MOSAIC), J. Geophys. Res., 113(D13), D13204, doi:10.1029/2007JD008782,
728 2008.
729
730 Zaveri, R. a. and Peters, L. K.: A new lumped structure photochemical mechanism for large-scale
731 applications, J. Geophys. Res., 104(D23), 30387, doi:10.1029/1999JD900876, 1999.
732
733 Zheng, B., Tong, D., Li, M., Liu, F., Hong, C., Geng, G., Li, H., Li, X., Peng, L., Qi, J., Yan, L.,
734 Zhang, Y., Zhao, H., Zheng, Y., He, K. and Zhang, Q.: Trends in China's anthropogenic
735 emissions since 2010 as the consequence of clean air actions, Atmos. Chem. Phys., 18(19),
736 14095–14111, doi:10.5194/acp-18-14095-2018, 2018.
737
738
739
740
741
742
743
744
745
746
747
748
749
750
751
752
753

https://doi.org/10.5194/acp-2019-875
Preprint. Discussion started: 8 November 2019

Atmospheric Chemistry and Physics Discussions

754 Table 1. Descriptions of simulations

Simulations	Descriptions
Control	Anthropogenic, biogenic and fire emissions are considered;
Industrial	Same as control except industry sector in anthropogenic emissions is excluded;
Residential	Same as control except residential sector in anthropogenic emissions is excluded;
Transportation	Same as control except transportation sector in anthropogenic emissions is excluded;
Power	Same as control except power sector in anthropogenic emissions is excluded;
Biogenic	Same as control except biogenic emissions are excluded;
Fire	Same as control except fire emissions are excluded;

755
756
757
758
759
760
761
762
763
764
765
766
767
768
769
770

https://doi.org/10.5194/acp-2019-875
Preprint. Discussion started: 8 November 2019

Atmospheric Chemistry and Physics Discussions

771 Table 2. Long range transport, local, and regional source contributions for seasonal mean O3
772 for different regions

	NCP	YRD	PRD	India
Winter	Outside: 81%	Outside:51%	Outside: 44%	Outside: 49%
	Local: 12%	Local: 26%	Local: 13%	N India: 35%
	NW China: 6%	NCP: 14%	YRD: 13%	S India: 16%
Spring	Outside: 73%	Outside:59%	Outside: 48%	Outside: 58%
	Local: 17%	Local: 24%	Local: 27%	N India: 28%
	NW China: 5%	NCP: 6%	YRD: 7%	S India: 14%
			SE China: 6%	
Summer	Outside: 51%	Outside:46%	Outside: 46%	Outside: 45%
	Local: 31%	Local: 32%	Local: 41%	N India: 38%
	NW China: 8%	SE China: 10%	SE China: 4%	S India: 17%
Autumn	Outside: 69%	Outside:61%	Outside: 50%	Outside: 42%
	Local: 21%	Local: 24%	Local: 15%	N India: 41%
	NW China: 7%	NCP: 8%	YRD: 11%	S India: 17%
			SE China: 10%	

773 (Outside sources include also transport from upper boundary of the model; NCP: Beijing, Tianjin, Hebei,
774 Shandong, and Henan; YRD: Anhui, Jiangsu, Shanghai and Zhejiang; SE China: Jiangxi, Fujian and Taiwan;
775 Central China: Hunan and Hubei; South China: Guangxi and Hainan)
776
777

https://doi.org/10.5194/acp-2019-875
Preprint. Discussion started: 8 November 2019

Atmospheric Chemistry and Physics Discussions

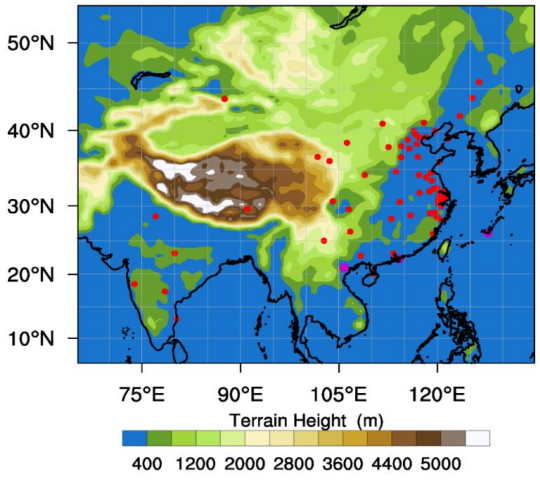

Fig. 1. WRF-Chem domain setting with terrain height and the locations of surface ozone observations marked by solid red circles. Purple solid circles mark the location of ozonesonde observations.

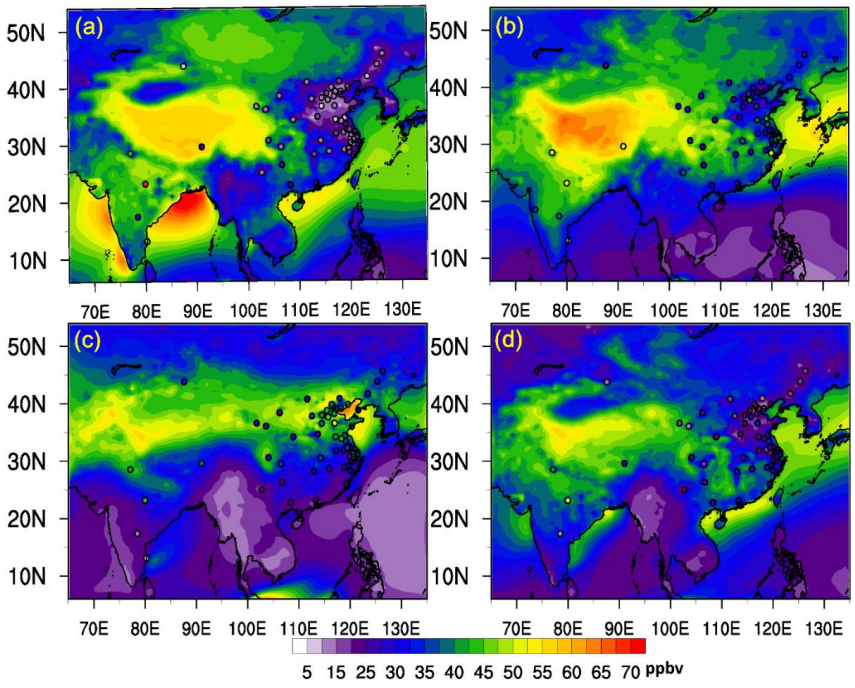

Fig. 2. Spatial distribution of simulated and observed seasonal mean ozone concentrations for Winter (a), Spring (b), Summer (c) and Fall (d).

https://doi.org/10.5194/acp-2019-875
Preprint. Discussion started: 8 November 2019

Atmospheric Chemistry and Physics Discussions

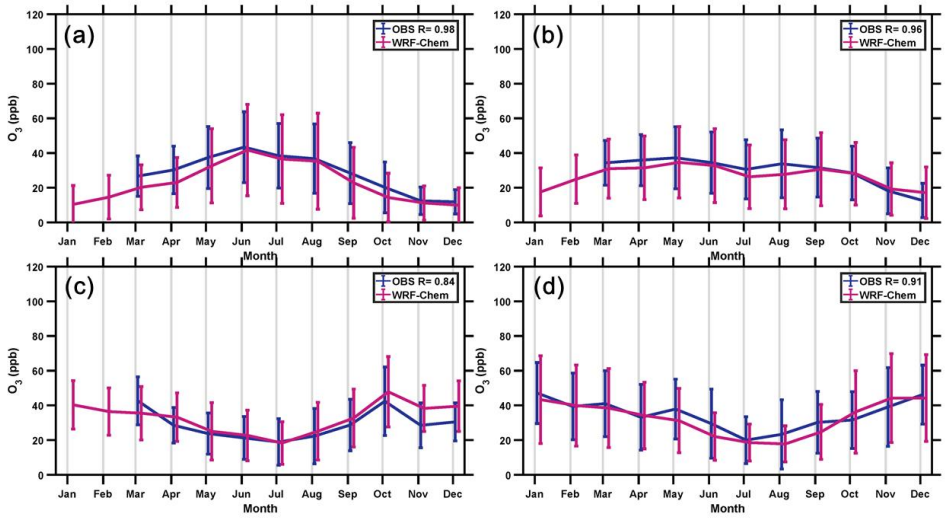

Fig. 3. Observed and simulated monthly mean O_3 concentrations averaged for the North China Plain (NCP) (a), Yangtze River Delta (YRD) (b), Pearl River Delta (PRD) (c), and India (d).

https://doi.org/10.5194/acp-2019-875
Preprint. Discussion started: 8 November 2019

Atmospheric Chemistry and Physics Discussions

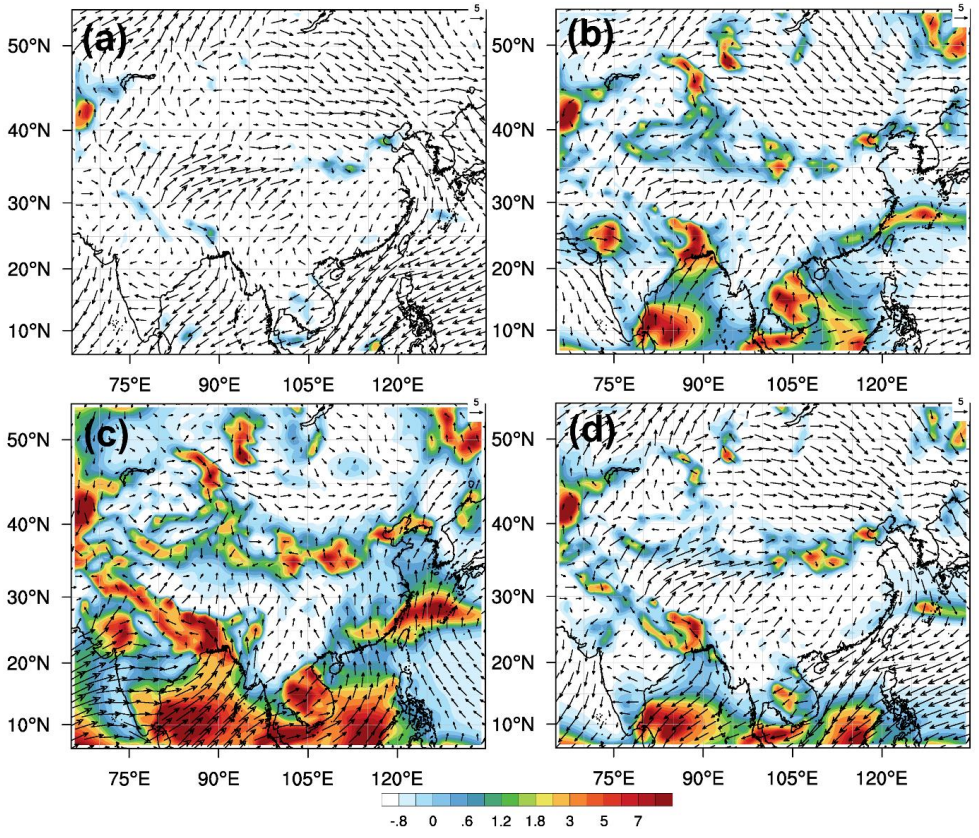

Fig. 4. Modeled mean near surface wind fields and the monsoon index in the boundary layer (0-1.5km) for winter (December, January, and February, a), spring (March, April, and May, b), summer (June, July and August, c), and autumn (September, October, and November, d)

https://doi.org/10.5194/acp-2019-875
Preprint. Discussion started: 8 November 2019

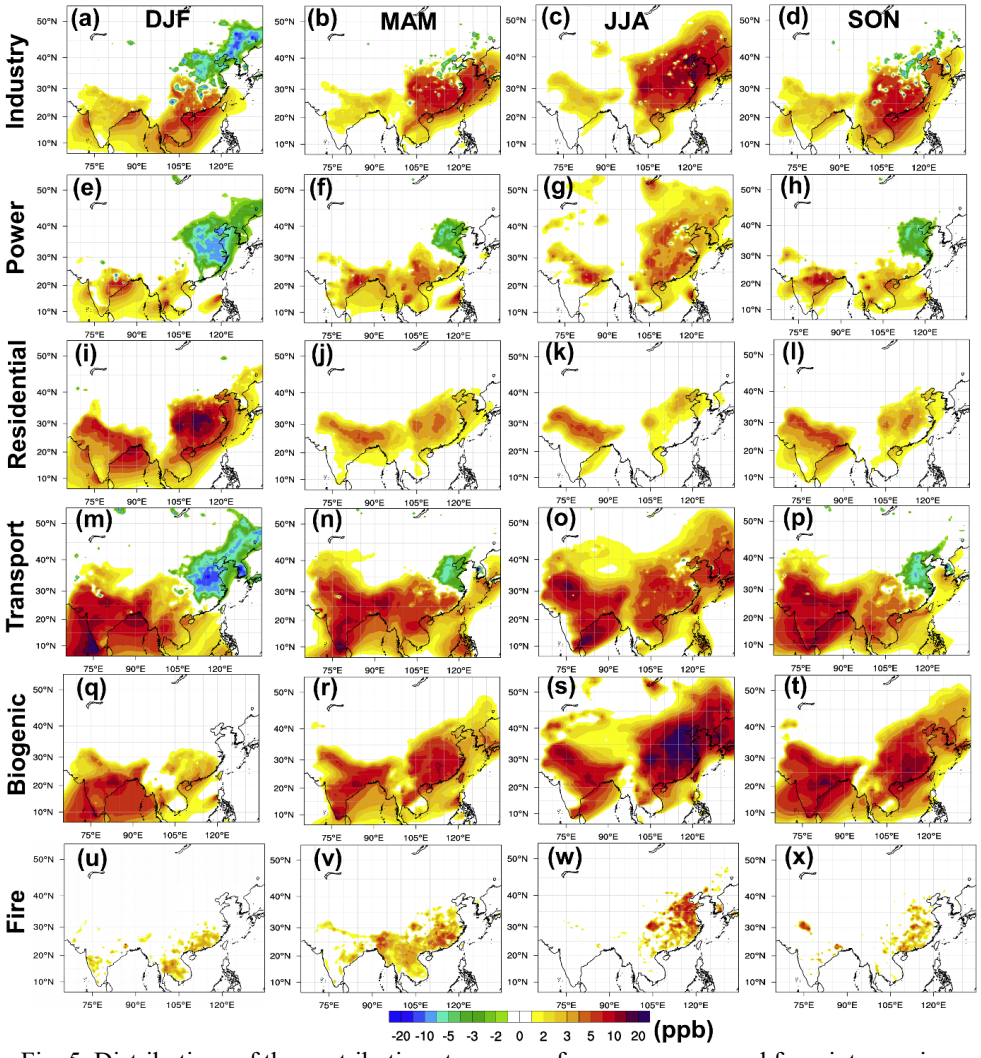

Fig. 5. Distributions of the contributions to near-surface ozone averaged for winter, spring, summer and autumn from industry (a-d), power, (e-h), residential (i-l), transport (m-p), biogenic (q-t) and fire (u-x) emissions.

https://doi.org/10.5194/acp-2019-875
Preprint. Discussion started: 8 November 2019

Atmospheric Chemistry and Physics Discussions

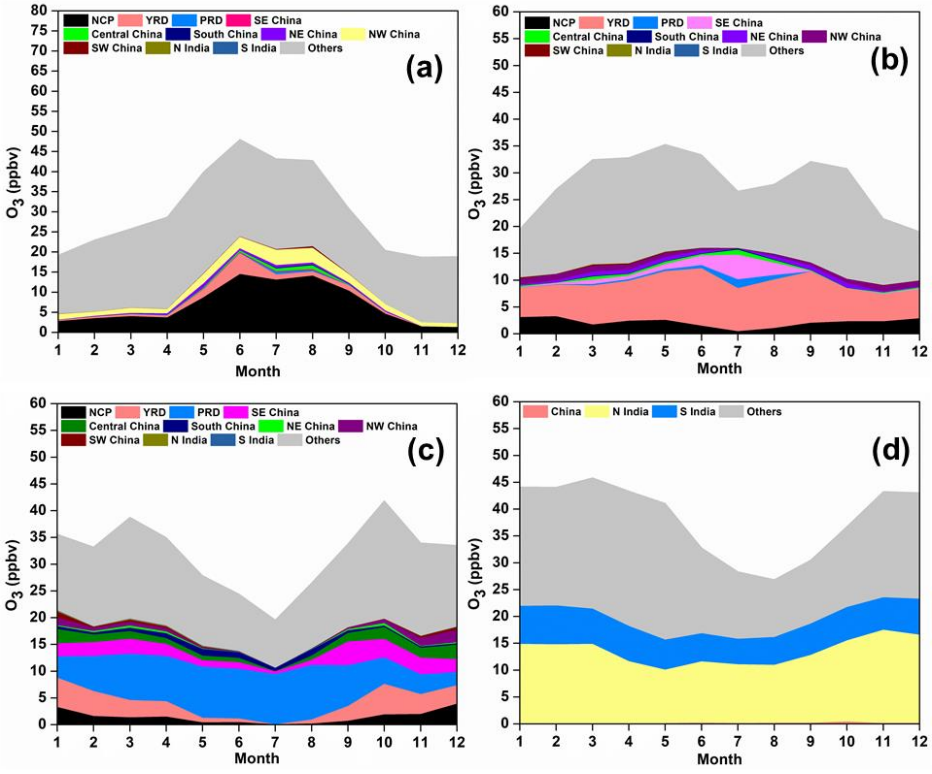

Fig. 6. Contributions to monthly mean ozone in NCP (a), YRD (b), PRD (c), and India (d) from different source regions (NCP: Beijing, Tianjin, Hebei, Shandong, and Henan; YRD: Anhui, Jiangsu, Shanghai and Zhejiang; SE China: Jiangxi, Fujian and Taiwan; Central China: Hunan and Hubei; South China: Guangxi and Hainan)